Scientific Journal of Impact Factor (SJIF): 5.71

e-ISSN (O): 2348-4470
p-ISSN (P): 2348-6406

International Journal of Advance Engineering and Research Development

Volume 5, Issue 05, May -2018

APPLICATION OF MONTE CARLO METHOD FOR DEVICES SIMULATION

Rajesh Kumar[1], Anjana Kumari[2], Tarun Kumar Dey[3]

[1]*University Department of Electronics, B.R.A Bihar University, Muzaffarpur -842001*
[1]*Department of Physics, N.D.College, Purnea -854301*
[3]*Post Graduate Department of Physics, L S College, Muzaffarpur -842001*

Introduction

The Monte Carlo method is a numerical statistical method that uses probability to solve physical and mathematical problems. This approach is well suited for simulation of physical phenomena associated with the stochastic processes. In fact, MC method was applied to some problems in the neutron transport and the statistical physics before it was applied to the carrier transport in semiconductor devices [1, 2]. MC simulations on transport properties are based on the description of particle motion. The progress in plasma simulations is helpful for the semiconductor device simulation [3].

The MC simulation of carrier transport has had a great progress over the past two decades. Researchers have implemented transport mechanisms in the device simulation, including new scattering processes, boundary conditions, electrostatic self-consistency, more comprehensive models, more efficient simulation algorithms, *etc*. The MC approach is regarded as the most important approach for the simulation of ultra-scale devices under the various electric field conditions. A more accurate simulation is the introduction of full energy electronic bands extracted by empirical pseudopotential calculations [4].

The first multi-valley MC simulation with the parabolic band, a single longitudinal acoustic (LA) phonon, and six fixed-energy intervalley phonons was introduced in ref. [5]. Ref. [6] considered the non-parabolic band and slightly altered phonon deformation potentials. Novel deformation potentials, which more closely match the available data on electron diffusion in silicon, are introduced in ref. [7] a few years later. This phonon model was the widely referenced review of the MC simulation, and it became the set of phonon energies and deformation potentials most often employed in the literature over the past two decades. Scattering with intervalley phonons are introduced by other workers [8]. The full band MC simulation of silicon, computed from empirical pseudopotentials, is firstly introduced in by Tand *et al*., [9]. They used the simple phonon model of LA phonons, six fixed intervalley phonons as ref. [4], and the deformation potentials of ref. [6]. The impact ionization in a full band MC simulation with the multi-valley deformation potentials of ref. [10] was introduced by Sano *et al.* [6]. Realistic MC device simulations using self-consistent full band were first performed by Fischetti *et al.* [11]. They also make the distinction between longitudinal and transverse acoustic (TA) phonon scattering, using a simple analytic dispersion for both LA and TA. Ref. [11] pointed out the definition of energy valleys in the full band simulation and used two phonon potentials, i.e. the fixed-energy optical phonon and the LA phonon including dispersion. The most sophisticated MC simulation for carrier transport in silicon was performed by ref. [12] and ref. [13]. They employed the full phonon dispersion obtained from an adiabatic bond-charge model and the full band computed from empirical pseudopotentials. The electron-phonon scattering rates were calculated as a function of wave vector and energy in consistency with the phonon dispersion and the band structure. Most MC simulations found in practice today employ full energy bands, yet scattering rates and energy exchange with the lattice are still computed with simplified phonon dispersion model. Phonon energies and deformation potentials in most frequent use are those originally introduced in ref. [7]. MC simulation is a huge computational simulation system that deals with the random events. Especially, the free flight time occupy a large part of the CPU time. Reduction of CPU time for this part of the simulation is a topic issue in MC simulation. Borsari employed the step scattering method to improve the simulation time [14]. Kato proposed to optimize the value of self-scattering, and the CPU time was further reduced significantly [15].

In this study, we employed the MC model which uses analytical descriptions for both the electron band structure and the acoustic phonon dispersion relationship, when the effect of heat generation is included in the simulation.

Procedure of Monte Carlo Method

General processes of the MC simulation for carriers transport and scattering in semiconductors devices have been well described [16]. This section provides a brief introduction for MC algorithm. Ensemble MC method used in this work preselects several tens of thousands “super-particles” to represent the mobile carriers inside the devices. This number is limited by computational constraints, but good simulation results can be obtained if the number of super-particles and simulation time are larger enough. The particles are initialized with thermal energy distributions by expression $3k_BT/2\times r$, r is a random number uniformly distributed between 0 and 1, and with randomly oriented wave vector. When the simulation is started, the particles are allowed to drift for short free flight time (τ), which is shorter than the average time between collisions, then one process of scattering is selected. The selection of scattering mechanism can be made in such

a way that the scattering rate compare to the total of all scattering rates (Γ) independent of the carrier energy. The free flight time (τ) of each particle can be consequently determined by total scattering rate (Γ) and a uniform random number (r_1) as [16]

$$\tau = -\frac{\ln(r_1)}{\Gamma} \tag{1}$$

The total scattering rate (Γ) is taken to be larger than the largest value of scattering rate $W_T(E_k)$ to avoid a negative value of scattering rate within the selected energy range of carrier. The MC simulations are not suited for low-field carrier transport, where the drift-diffusion method may be preferred. However, the MC method

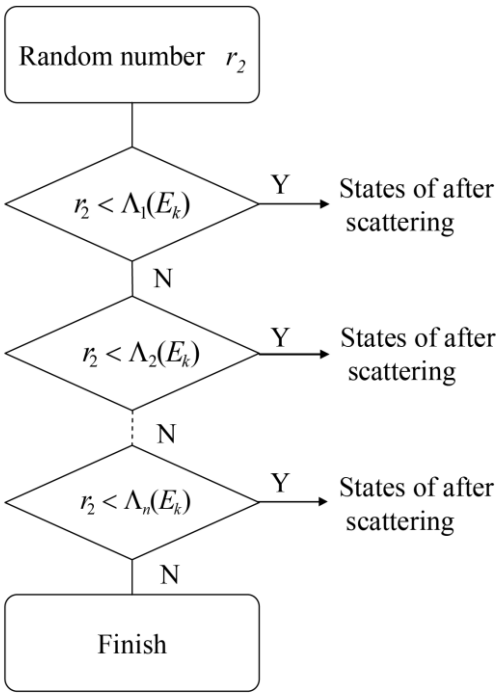

Figure1 Selection of a scattering mechanism algorithm flowchart.

represents the most physically comprehensive simulation approach for charge transport in semiconductors.

Drift Process

When potential energy of carriers varies slowly as a function of position, drift process of carriers in semiconductor devices can be treated semi-classically. Thereby, carriers can be regarded as free particles with an effective mass. Based on the equations of motion for carriers the change in the wave vector during the free flight time τ is obtained by integrating the equation of motion with respect to time; thus [16],

$$\Delta k = -\frac{1}{\hbar}\int_t^{t+\tau} \nabla H dt \tag{2}$$

where H is the total energy of an carriers with a charge e given by

$$H = E_k - eV(r) \tag{3}$$

where E_K is the kinetic energy of the carriers and $V(r)$ is the electrostatic potential. If an electric field $\boldsymbol{F}$ is applied on a semiconductor device, Eq. (4.2) has a solution as:

$$\Delta k = -\frac{eF}{\hbar}\tau \tag{4}$$

Scattering Process

In the scattering process, firstly determined what scattering mechanism by which a carrier is to be occurred, and then identify the carrier state after the scattering. The selection of a scattering mechanism can be made by using functions $\Lambda_n(E_k)$ defined as [16]:

$$\Lambda_n(E_k) = \frac{\sum_{j=1}^{n} W_j(E_k)}{\Gamma} \qquad \text{For } n = 1, 2, \ldots, N \tag{5}$$

which are the successive summations of the scattering rates normalized with the maximum of sum of all scattering rates Γ. Γis identical to the parameter defined by

$$\Gamma = Max(\sum_{j=0}^{n} W_j(E_k)) \quad (6)$$

and n is the total number of scattering mechanisms. A scattering mechanism for carriers with energy E_k is selected by generating a random number r_2 lying between 0 and 1, and comparing r_2 to $\Lambda_n(E_k)$; if the functions $\Lambda_n(E_k)$ is satisfied the condition as follows:

$$\Lambda_{n-1}(E_k) < r_2 < \Lambda_n(E_k) \qquad n = 1, 2, \ldots, N \qquad 0 \quad (7)$$

n-th scattering mechanism is chosen. The Pauli's exclusion principle is not taken into account in Eq. (7), because the carrier occupancy in the final states is ignored. Selection steps for scattering are described in the flowchart shown in Figure 1.

Velocity Calculation

In simulation of semiconductor device, MC simulation is equivalent to solving the Boltzmann transport equation. Distribution function can be calculated by the mean velocity of carriers, and energy can be calculated when the flight time of carriers in each volume element of k-space is accumulated. This process demands a large amount of memory to accumulate the data in k-space. However, it is not necessary to do this, due to the mean values of carrier velocity and carrier energy can be calculated directly by monitoring each carrier flight and then taking an average over all flights. The instantaneous carrier velocity is formed by [16]

$$\upsilon = \frac{1}{\hbar}\nabla_k E_k \quad (8)$$

therefore, the mean velocity of carrier during flight time τ can be formed as

$$<\upsilon>_\tau = \frac{1}{\hbar}\frac{\nabla E_k}{\nabla k} \quad (9)$$

where ∇E_k and ∇k are small increments of the carrier energy and carrier wave vector during flight time τ, respectively. Substituting Eq. (4) into Eq. (9), then

$$<\upsilon>_\tau = -\frac{\nabla E_k}{eF\tau} \quad .....(10)$$

Making use of the mean velocity of carrier during flight time τ given by Eq. (10), the mean velocity of carriers during the total simulation time T is given as

$$<\upsilon>_T = \frac{1}{T}\sum <\upsilon>_\tau \tau = \frac{1}{eFT}\sum (E_f - E_i) \quad (11)$$

where E_f is the energy of carrier at the end of the flight and E_i is the energy of carrier at the start of the flight. The summation has to be made for all free flights. Eq. (11) shows that the energy increment during each free flight time. The same reasoning leads to mean energy of carrier being given as follows

$$<E>_T = \frac{1}{T}\sum <E>_\tau \tau \quad (12)$$

where <E> is given to a good approximation by

$$<E>_\tau = \frac{E_i + E_f}{2} \quad (13)$$

Monte Carlo Device Simulation

MC method for device simulation has similar procedure with the EMC simulation. Only a few elements have to be added for MC device simulation. Carriers spread in a boundary less bulk semiconductor; however, transports of carrier are restricted by the boundary condition. Therefore, to set up suitable boundary conditions, it is necessary for carriers to reach the surface of the device [16]. Carriers should either be “exit” or “enter” the ohmic contact area of the device or might “reflected” at the insulator surface of the device during the simulation. Self-consistently potential and electric field calculation with the distribution of carriers through the solution of the Poisson equation with appropriate boundary conditions is other thing to be taken into account in device simulation. Boundary conditions applied to the carrier motion and the Poisson equation must be consistent each other. Therefore, the calculation of carrier motion with suitable boundary conditions, the self-consistent Poisson calculation with charge distribution, and the treatment of carrier

associated with the delete, exit or entrance of carrier through the surface of the device are necessary arrangements in the Monte Carlo device simulations.

Figure 2 shows a typical flowchart of the Monte Carlo device simulation. The geometry of the device, the material composition, layer structure, the apply voltage, the doping profile, and the contact regions are specifies in step "physical system" according to the data given by the user.

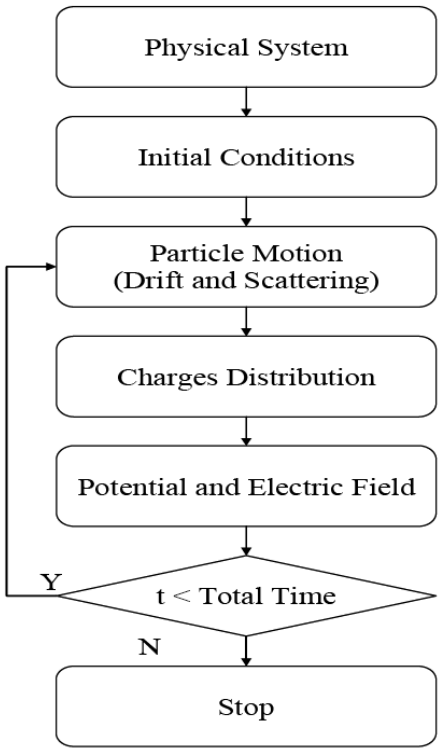

Figure 2 . Basic Monte Carlo algorithm flowchart.

The initial carrier distribution in real space and *k*-space, and the initial potential profile in the device are specifies in the subroutine "initial condition". The number of carrier is always varying during the simulation because carriers are exit or enter in ohmic contact region of device. The profile of carrier density calculated from particle distribution in subroutine "charge distribution". The profile of the carrier density obtained is transferred to the subroutine "potential and electric field" for the potential and electric field calculation. The role of each subroutine is described in following subsections.

Initial Condition

At the start of the simulation, the initial condition of device as the particle distribution in real space and *k*-space, and the potential profile are specifies in the subroutine "initial condition".

The carriers are usually distributed in spatial accordance with the density profile of the corresponding doping concentration. The particles may be distributed spatially according to the density profile of carriers for save computing time, which is computed in advance by a device simulation based on the drift-diffusion method.

The initial distribution of carrier's energy is determined by random numbers based on the assumption that the energy of carrier is nearly at the thermal equilibrium at the start of the simulation. Thus, the energy of each carrier E_k is calculate by [16]

$$E_k = -1.5 \cdot k_B T \ln(r) \quad \text{.....(14)}$$

where k_B is the Boltzmann constant, T is the lattice temperature (assumed to equal the carrier temperature), r is random number uniformly distributed between 0 and 1. The wave vector k of carrier can be determined by the *Ek-k* relation based on the energy value given by Eq. (13). Due to the energy of carriers is located at minimum point of real band structure, the simple spherical and parabolic band can be assumed, the k vector is determined by the relation

$$k = \frac{\sqrt{2m^* E_k}}{\hbar} \quad \text{.....(15)}$$

For non-parabolic bands, the energy of carrier is correct use the *Ek-k* relation given by Eq. (2). Then, Eq. (14) has new form as follows:

$$k = \frac{\sqrt{2m^* E_k(1+\alpha E_k)}}{\hbar} \quad \text{.....(16)}$$

For ellipsoidal, parabolic bands, the components of **k** are obtained by a similar procedure using Eq. (15).

Charge Distribution

The density profile of carrier is directly related to the particle distribution in the device. The calculation of the density profile of carrier is simple and is based on counting the number of particles for each grid point. The simplest "nearest-grid-point method" is usually employed in the MC device simulation, in which the density profile of carrier at a grid point (i, j) is calculated from the total number of particles in the cell surrounding the grid point as shown in Figure 3. Since the particles are regarded as super-particles in the calculation, the carrier density is obtained as [16]

$$n(i,j) = N(i,j) \times \frac{N_{pp}}{\Delta x \Delta y} \quad \text{.....(17)}$$

where N_{pp} is the number of carriers per super-particle, $N(i, j)$ is the number of particle in the cell (i, j), and $\Delta x\Delta y$ is the square of the cell for the case of the two-dimensional device.

There is inevitably statistical noise in the distribution of carrier profile since the number of particles employed is rather limited. The statistical noise may lead to numerical instability in some cases. Such statistical noise can be avoided using the cloud-in-cell method. In the cloud-in-cell method, the carrier associated with a particle is regarded as a cloud of carrier spread spatially. We report a brief description of the "cloud-in-cell" method in follow.

The finite difference mesh is considered with the nodes located at (x_i, y_j). The constant spatial step in the x-direction and y-direction are denote by Δx and Δy, respectively. Then, if (x, y) the point coordinates in which one wants to compute the density of carrier, with $x_i < x < x_i+1$ and $y_i < y < y_i+1$, the density of carrier is compute in the following way

$$n(i,j) = \frac{N(i,j)}{A^2(i,j)}(x_{i+1} - x)(y_{j+1} - y)$$

$$n(i+1,j) = \frac{N(i+1,j)}{A^2(i+1,j)}(x - x_i)(y_{j+1} - y)$$

$$n(i,j+1) = \frac{N(i,j+1)}{A^2(i,j+1)}(x_{i+1} - x)(y_{j+1} - y)$$

$$n(i+1,j+1) = \frac{N(i+1,j+1)}{A^2(i+1,j+1)}(x - x_i)(y - y_j) \quad \text{.....(18)}$$

where $A(i, j) = \Delta x\Delta y$. The cloud-in-cell method do exist that avoid the problems of self-forces but they are necessary when deal with heterostructures and the spatial step is not regular. The cloud-in-cell method reduces the amplitude of fluctuation in the density profile of carrier during the simulation because of the spreading of the carrier cloud. However, when the cloud-in-cell method is applied to a device with abrupt heterojunction, the carrier density obtained by the "cloud-in-cell" scheme may be over-estimated on one side of the junction and under-estimated on the other side.

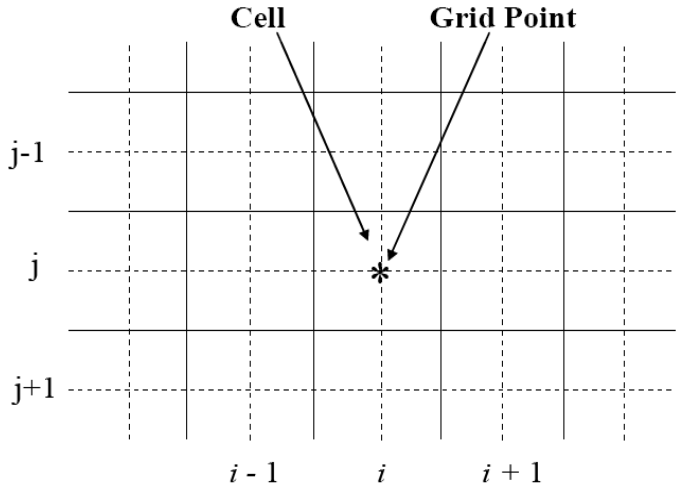

Figure 3 Cell and grid point.

Solution of Poisson Equation

MC device simulation requires potential profiles extracted from self-consistent solution of the Poisson equation. Analytical solution for the Poisson equation is hardly accepted in a realistic device structure with appropriate boundary conditions, due to the potential profile has to be determined for a large number of charged particles. Finite difference scheme of the Poisson equation with one- or two-dimensional form is an effective method among various numerical methods.

Poisson equation can be solved by the following form

$$\nabla \cdot [\varepsilon(x)\nabla \phi(i, j, t)] = -q[N_D(i, j) - N_A(i, j) - n(i, j, t) + p(i.j, t)] . \quad (19)$$

There are two sources of charge in Eq. (19): mobile charge and fixed charge. Mobile charges are electrons and holes, whose densities are represented by *n* and *p*. Fixed charges are ionized donor and acceptor atoms whose densities are represented by N_D and N_A, respectively. ε is the permittivity of material. The subscripts (*i*, *j*) denote the (*i*, *j*)-th grid on the *x*-*y* plane. The discretization of the Poisson will give an algebraic system to solve if the two-dimensional regular finite-difference grid is applied. But this method is quite complicated to solve, because the boundary conditions are difficult to implement in a generic simulation. Furthermore, this algebraic system is consuming from the grid view of computer memory.

In this section, non-stationary Poisson equation will be introduces. This equation is easy to solve and can be implemented in a general numerical context with robust and numerical schemes. The form of the non-stationary Poisson equation is shown in the following

$$\frac{1}{k_S}\frac{\partial \phi}{\partial t} + \nabla \cdot [\varepsilon(i, j)\nabla \phi(i, j, t)] = -q[N_D(i, j) - N_A(i, j) - n(i, j, t) + p(i, j, t)] , \quad (20)$$

where the variables (*n*, *p*, N_D, N_A , ε) have the same meaning as above. k_S is a constant giving the right dimensions of the potential term $\frac{\partial \phi}{\partial t}$. The solution of this equation is similar with those from classical Poisson equations described in the precedent paragraph. Furthermore, both solutions have the same initial potential conditions and the same boundary conditions. Therefore, once Eq. (20) is numerically solved, classical Poisson equation will be easily solved by simply getting the solution of the non-stationary Poisson equation for big final time.

In the context of finite difference method, same numerical scheme is obtained applying finite-difference method of derivatives to the non-stationary Poisson equation. In the finite difference method, the value of the potential on the grid points can be discretized on an equally spaced mesh as

$$\nabla^2 \phi(i, j, t^n) = \frac{\phi^n_{i+1,j} - 2\phi^n_{i,j} + \phi^n_{i-1,j}}{\Delta x^2} + \frac{\phi^n_{i,j+1} - 2\phi^n_{i,j} + \phi^n_{i,j-1}}{\Delta y^2} \quad (21)$$

where the Δ*x* and Δ*y* are the spatial mesh size. The $\phi^n_{i,j}$ is the potential computed at time $t^n = t_i + n\Delta t$, in the point (*i*, *j*). Applying these expressions to the non-stationary Poisson equation, one gets the following numerical form [17]

$$\phi^{n+1}_{i,j} = \phi^n_{i,j} + \Delta t(-\varepsilon_{i,j}(\frac{\phi^n_{i+1,j} - 2\phi^n_{i,j} + \phi^n_{i-1,j}}{\Delta x^2} + \frac{\phi^n_{i,j+1} - 2\phi^n_{i,j} + \phi^n_{i,j-1}}{\Delta y^2}) - q[N_D(i, j) - N_A(i, j) - n^n_{i,j} + p^n_{i,j}] \quad (22)$$

The presented scheme is valid only in the case of homogeneous case, but it is easy to expand it to the heterogeneous structures. Due to the fact that the initial conditions and the boundary conditions are included in the presented scheme, it is easy to implement this solution in simulation of semiconductor devices.

Electric Field Calculation

It is easy to get the solution of the electric field of device system by the solution of the static Poisson equation or the non-stationary Poisson equation. The generic definition of the electric field is as follows [16]

$$E(x, y) = -\nabla \phi(x, y) \quad (23)$$

So, in the context of finite-difference method, the solution of electric field in the two dimensional cells of the grid as follows:

$$E_x(i, j) = -\frac{\phi_{i+1,j} - \phi_{i-1,j}}{2\Delta x}$$

$$E_y(i, j) = -\frac{\phi_{i,j+1} - \phi_{i,j-1}}{2\Delta y} \quad .....(24)$$

These simple expressions are used in simulation. Although the expressions are simple, but the result values of electric field are accurate and robust.

Conclusion

Details of the application of the Monte Carlo methods to device simulation have been described in this chapter. Calculated results on carrier transport or performance of devices may not precisely agree with experimental results due to uncertainty in the knowledge of material parameters or scattering mechanism. However, the error in the MC simulation of semiconductor devices is acceptable for many cases. The present approach is more than an order of magnitude faster than the full-band device simulation, and is accessible on modern computers. Monte Carlo simulations with non-parabolic bands can be applied to the engineering of low-voltage nanoscale devices and materials, where detailed knowledge of carrier transport including the electron-phonon interaction is required.

References

[1] B. T. Browne, J. J. H. Miller, *Numerical Analysis of Semiconductor Devices and Integrated Circuits*, Boole Press, Dublin 1981.
[2] M. Kurata, *Numerical Analysis for Semiconductor Devices*, Lexington Press, Lexington, Mass 1982.
[3] M. S. Mock, *Analysis of Mathematical Models of Semiconductor Devices*, Boole Press, Dublin 1983.
[1] Yu. A. Shreider, *The Monte Carlo Method*, Pergamon, Oxford, 1956
[2] K. Binder, *Application of the Monte Carlo Method in Statistical Physics*, Springer,Berlin, 1984
[3] R. W. Hockney and J. W. Easwood, *Computer Simulation Using Particles*, Mc Graw-Hill, New York 1981.
[4] J. Y. Tang and K. Hess, "Impact ionization of electrons in silicon (steady state)", J.Appl. Phys. **54**, no. 9, 5139 (1983).
[5] C. Canali, C. Jacoboni, F. Nava, G. Ottaviani, and A. Alberigi-Quaranta, "Electron drift velocity in silicon", Phys. Rev. B **12**, no. 4, 2265 (1975).
[6] C. Jacoboni and L. Reggiani, "The Monte Carlo method for the solution of charge transport in semiconductors with applications to covalent materials", Rev. Mod. Phys. **55**, no. 3, 645 (1983).
[7] R. Brunetti, C. Jacoboni, F. Nava, and L. Reggiani, "Diffusion coefficient of electrons in silicon," J. Appl. Phys. **52**, no. 11, 6713 (1981).
[8] T. Yamada, J.-R. Zhou, H. Miyata, and D. K. Ferry, "In-plane transport properties of Si/Si1−xGex structure and its FET performance by computer simulation", IEEE Trans. Electron Devices **41**, 1513 (1994).
[9] J. Y. Tang and K. Hess, "Impact ionization of electrons in silicon (steady state)", J. Appl. Phys. **54**, no. 9, 5139 (1983).
[10] C. Canali, C. Jacoboni, F. Nava, G. Ottaviani, and A. Alberigi-Quaranta, "Electron drift velocity in silicon", Phys. Rev. B **12**, no. 4, 2265 (1975).
[11] M. V. Fischetti and S. E. Laux, "Monte Carlo analysis of electron transport in small semiconductor devices including band-structure and space-charge effects", Phys. Rev. B **38**, no. 14, 9721 (1988).
[12] P. D. Yoder and K. Hess, "First-principles Monte Carlo simulation of transport in Si", Semicond. Sci. Technol. **9**, 852 (1994).
[13] T. Kunikiyo, M. Takenaka, Y. Kamakura, M. Yamaji, H. Mizuno, M. Morifuji, K.Taniguchi, and C. Hamaguchi, "A Monte Carlo simulation of anisotropic electron transport in silicon including full band structure and anisotropic impact-ionization model", J. Appl. Phys. **75**, no. 1, 297 (1994).
[14] V. Borsari and C. Jacoboni, "Monte Carlo Calculations on Electron Transport in CdTe", Phys. Status Solidi B **54**, 649 (1972).
[15] K. Kato, "Hot-carrier simulation for MOSFETs using a high-speed Monte Carlo method", IEEE Trans. Electr. Dev., ED **35**, 1344 (1988).
[16] E. Pop, R. W. Dutton, and K. E. Goodson, "Analytic band Monte Carlo model for electron transport in Si including acoustic and optical phonon dispersion", J. Appl. Phys. **96**, 4998 (2004).
[17] K. Tomizawa, *Numerical simulation of submicron semiconductor devices*. Artech House, 1993.

